

Thermally-Driven Nanoparticle Array Growth from Atomic Au Precursor Solutions

Shunji Egusa,^{†,§} Peter L. Redmond,[‡] and Norbert F. Scherer^{*,‡}*Departments of Physics and Chemistry, The James Franck Institute, The University of Chicago,
929 East 57th Street, Chicago, Illinois 60637**Received: August 21, 2007; In Final Form: October 24, 2007*

We observe spontaneous formation of hexagonal and square arrays of sub-10-nm Au nanoparticles by asymmetric heating of a novel precursor material, alkanethiol-passivated atomic Au cluster solutions, on amorphous carbon films. Nanoparticle shape, array symmetry, and lattice constant are controlled by substrate temperature and solvent composition. It is shown that definition of the array lattice points precedes complete particle formation, ruling out an entropy-driven “hard sphere”-type self-assembly process. Mechanisms for monolayer array formation are discussed.

Introduction

The unique properties of metallic nanoparticles^{1,2} have potential to impact optical frequency communication/computation technology,^{3,4} biomedical labeling,^{5,6} and chemical catalysis.^{7,8} Realization of such applications requires control over the assembly of nanoparticles, as well as particle shape and size. Various approaches for array formation exist, including both self-assembly and lithography methods. The solvent drying-mediated self-assembly method of nanoparticle array formation gives impressive results but only with highly monodisperse constituent nanoparticles with typically less than a few percent standard deviation in size.^{9–11} It also requires slow evaporation and careful control of the sample environment. The “nanosphere lithography” method uses layers of self-assembled polystyrene beads to create a mask for lithographic definition of the particle array.^{12,13} Although versatile, this method like many other lithographic techniques^{14–16} does not readily form arrays with lattice constants in the sub-10 to 50 nm regime. The present report describes a simple approach for creating ordered two-dimensional Au nanoparticle arrays achieved by relatively fast solvent evaporation, asymmetric heating, and a novel precursor material of atomic Au clusters. Two-dimensional square lattices of square Au nanoparticles and close-packed hexagonal lattices of spherical Au nanoparticles are controllably obtained with this method. Solvent composition and substrate temperature are shown to control the array symmetry and lattice constant.

Experimental Section

Dodecanethiol passivated atomic Au clusters were used as the precursor for array formation.¹⁷ These atomic Au clusters are chemically stable making them suitable for synthesis. Moreover, the clusters are highly fluorescent and robust

chromophores (i.e., resistant to photobleaching).^{18,19} Preparation of atomic Au clusters is described in detail elsewhere.¹⁷ Briefly, 6-nm-diameter Au particles were synthesized using a standard literature protocol (see Figure 1 inset).^{20,21} Clusters were formed by refluxing the 6-nm-diameter Au particles in a dioctyl ether (bp = 290 °C) solution of dodecanethiol (10:1 volume ratio of dioctyl ether to dodecanethiol). The Au cluster ultraviolet–visible (UV–vis) absorption spectrum shown in Figure 1 exhibits an extremely sharp electronic transition at $h\nu = 4.1$ eV (line width $\Gamma = 0.20$ eV) that gives a luminescence spectrum centered at 3.6 eV. We estimate the emission quantum yield to be $>40\%$.²² The cluster absorption spectra differ entirely from that of the starting Au nanoparticle solution. The final refluxed solution was devoid of residual Au nanoparticles, confirmed by the absence of the surface plasmon absorption peak at $h\nu = 2.4$ eV ($\lambda = 520$ nm), and transmission electron microscopy (TEM). Atomic Au cluster solutions in octanethiol and dodecanethiol gave essentially identical absorption spectra (after correction for solvent absorption) supporting the idea that atomic Au cluster formation is unaffected by the alkanthiol length.

Nanoparticle arrays were formed by diluting dioctyl ether solution of atomic Au clusters (0.1 wt %) with toluene²³ and depositing 1 μ L of the resultant solution on an amorphous carbon film TEM grid (3 mm diameter). The grid was immediately placed on a hot plate and heated in otherwise ambient conditions until the solvent evaporated. Dilution ratios, substrate temperatures, and heating times were varied exploring the range of structures formed and to gain insight into the mechanism for nanoparticle array formation.

Results

Hexagonal Au nanoparticle arrays formed on the TEM grid when a 1:2 [dioctyl ether]/[toluene] diluted atomic Au cluster solution was heated to evaporation at 95 °C. Figure 2A shows the hexagonal lattice with a particle size of 5.8 ± 0.4 nm and a lattice constant of 9.0 ± 0.1 nm. No other array symmetries were found on the grid. Figure 2B demonstrates the high degree

* Corresponding author. E-mail: nfschere@uchicago.edu.

[†] Department of Physics.

[‡] Department of Chemistry.

[§] Current address: Department of Materials Science and Engineering, Massachusetts Institute of Technology, 77 Massachusetts Avenue, Cambridge, MA 02139-4307.

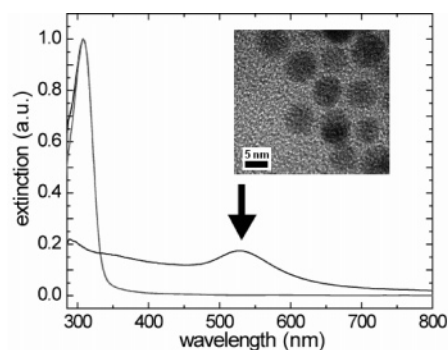


Figure 1. UV-vis extinction spectra of Au cluster solutions in dioctyl ether, prepared with octanethiol and dodecanethiol, show the same absorption peak around 305 nm. The spectra were measured with toluene dilution. The background absorption by dioctyl ether and alkanethiols was subtracted. The arrow indicates the particle plasmon absorption of the nanoparticle solution before digestion. Inset: TEM image of ~ 6 -nm-diameter dodecanethiol passivated particles.

of order obtained in the hexagonal array; the Fourier image shows well-defined spots to second order. When the same (diluted) solution was heated to evaporation at 105 °C, a square lattice of square Au nanoparticles was formed with a particle edge length of 10.5 ± 0.8 nm and a lattice constant of 11.4 ± 0.2 nm (see Figure 2D). A third morphology, Au nanowires with a width of 3 nm and length of up to 1 μ m, were found coexisting with hexagonal lattices of spherical particles when the substrate was heated at 100 °C for 6 min (Figure 2E). Figure 2F shows the distribution of nanoparticle sizes within the arrays pictured in Figure 2C and D. The histograms²⁴ are reasonably narrow: the widths are less than 8% of the mean values.

Both substrate temperature and dilution ratio affect the array symmetry. Figure 3A is a phase diagram for array formation with respect to substrate temperature and dilution ratio. The dilution ratio, D , is defined as $D = V_{\text{ether}}/(V_{\text{ether}} + V_{\text{toluene}})$, where V_{ether} is the volume of dioctyl ether and V_{toluene} is the volume of toluene. Figure 3B shows that the lattice constant depends strongly on the dilution ratio. As D is decreased from 1.0 to 0.2, the hexagonal lattice constant decreases from 13.7 to 5.8 nm ($T = 95$ °C). With $D \leq 0.1$ only randomly scattered particles were observed.

To determine if the cluster concentration affects array formation, the atomic Au cluster concentration was varied by diluting the cluster solution with dioctyl ether and then adding an equal volume of toluene (i.e., keeping $D = 0.5$). The Au cluster concentration in dioctyl ether was varied from 0.1 wt % to 0.02 wt % with ~ 0.02 wt % intervals; each solution gave similar lattice constants. Therefore, the array lattice constant does not depend on the concentration of Au clusters.

It is possible that the atomic Au clusters first nucleate in solution and then deposit onto the grid. To test this, 1 mL of Au cluster solution was diluted with 1 mL of toluene and heated at 100 °C in a flask to evaporation. The remaining brown residue was redispersed in 1 mL of toluene by sonication. Large polydisperse nonuniformly shaped nanoparticles were found in the resultant solution as determined by TEM imaging of aliquots. This suggests that the clusters do not nucleate/grow in solution and subsequently deposit on the surface. Instead, the nanoparticle arrays appear to form by Au cluster nucleation on the carbon substrate. However, simply allowing the atomic Au cluster solution to evaporate at room-temperature yields no nanoparticles on the grid (see Figure 4A). Thus, array formation requires elevated substrate temperature. To further test if the particles “grow” on the surface or simply deposit as whole particles,

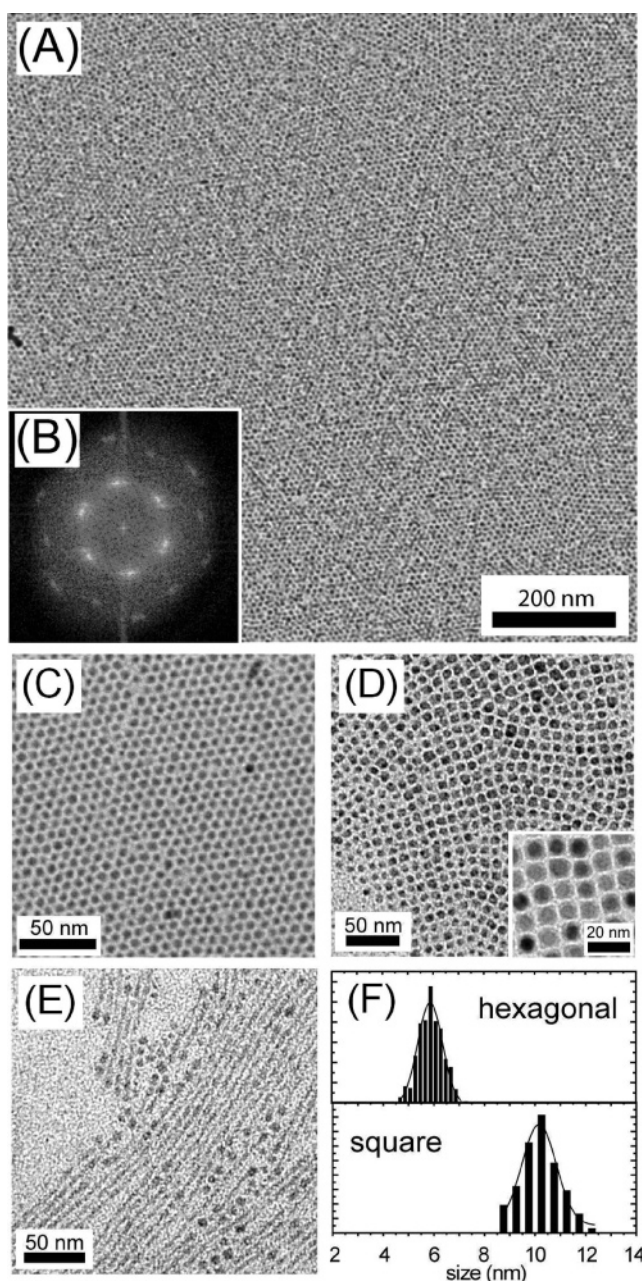


Figure 2. (A) Two-dimensional hexagonal Au nanoparticle lattice. (B) A 2D Fourier transformation of the entire image (A). (C) Magnified section of A. (D) Square Au nanoparticle lattice. (E) Au nanowires. (F) Histogram of particle sizes for the hexagonal (particle diameter = 5.8 ± 0.4 nm) and square lattice (diameter = 10.5 ± 0.8 nm) constructed from 300 particles in the TEM images. The solid line shows a Gaussian best-fit.

cluster solutions were heated for 4 min on grids then removed from the heat and allowed to cool to room temperature. TEM imaging of the sample (Figure 4B) showed that the shorter heating time yielded underdeveloped particles but already formed in a clearly defined hexagonal lattice. This shows that the definition of lattice points precedes complete nanoparticle formation. This conclusion is in contrast to the solvent drying-mediated method where whole particles deposit from solution onto a surface thus defining the lattice.

The array lattice constant is not significantly affected by the alkanethiol length. Hexagonal lattices were obtained for each Au cluster solution (lattice constants: octanethiol = 8.5 ± 0.7 nm, dodecanethiol = 9.0 ± 0.1 nm) after 6 min of heating on a grid with $T = 95$ °C. Thus, the mechanism of array

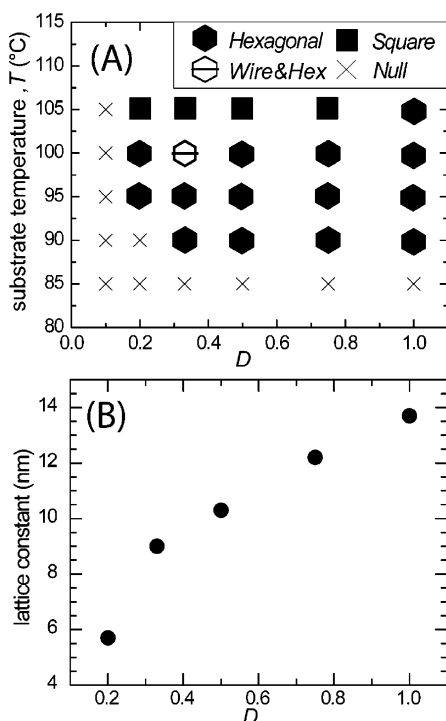


Figure 3. (A) Plot of lattice symmetry as determined by the dilution ratio, D , and substrate temperature. “Wire&Hex” indicates the formation of wires coexisting with spherical particles in a hexagonal array. “Null” indicates that no ordered structures were found. (B) A plot of the hexagonal lattice constant vs the dilution ratio, D .

formation depends primarily on the substrate temperature and dilution ratio.²⁵

Discussion

Solvent drying-mediated self-assembly can be modeled as a solution of hard spheres that undergoes an entropy-driven disorder to order transition when the sphere volume fraction becomes large.^{26–28} This mechanism does not apply here because the lattice point definition precedes complete nanoparticle formation during array development. One possible mechanism for array formation involves the Bénard–Marangoni effect, wherein a thin fluid layer heated from below supports formation of stable spatial convection patterns when the liquid temperature gradient exceeds a critical value.^{29–32} Although the effect has been shown to form micrometer-sized hexagonal morphologies in thin polymer films,^{33–35} it is unclear if the effect can extend to the present size regime (~ 10 nm lattice constant).^{36–38} At present, our results are not sufficiently restrictive to prove that nonequilibrium fluid flow dynamics

alone can give rise to the aforementioned mechanism of lattice point and lattice symmetry formation followed by in situ nanoparticle formation.

We consider a second possible mechanism involving the temperature-dependent nature of the Au–thiol bond.³⁹ Au(111) surfaces covered by SAMs of dodecanethiol molecules have been shown to form ordered structures when heated in variable-temperature STM experiments.^{40,41} Guo and co-workers noticed the appearance of a “zebra-stripe” phase associated with the reconstruction of the gold substrate when the sample was heated to above 90 °C.⁴⁰ Furthermore, the phase change was initiated by a relatively small temperature change of ~ 5 °C. In our experiments, it is possible that the Au clusters uniformly coat the surface (Figure 4A). Once the solution has evaporated (or in the final phase of evaporation), the elevated temperature causes a structural self-organization process facilitated by the dodecanethiol molecules thus forming particle arrays.

A third possible mechanism relies on the amphiphilic nature of the Au cluster (i.e., an Au core and alkane chain “surfactant”) for array formation. Amphiphilic molecules with asymmetric or dipolar interactions, including copolymers, are known to self-organize into hexagonal symmetry or stripe patterns depending on the temperature and the composition of the system.^{42,43} Specifically, an operative process could be analogous to the “liquid crystal template mechanism”⁴⁴ of silica-surfactant composites, where the solvent evaporation-driven volume fraction change causes phase separation and creates surfactant liquid crystal structures that serve as organic templates to form ordered inorganic structures.

It is also possible that there is a synergy of the aforementioned mechanisms; particle array formation results from contributions of each of the above mechanisms. Hosoi et al. modeled the self-assembly of nanometer-sized (10–100 nm) two-dimensional hexagonal and stripe arrays of diblock copolymers. They found that array formation can be described by the relative contributions of four effects: Marangoni forces, solvent evaporation, polymer–polymer interactions, and polymer diffusion.⁴⁵ In this context, dilution with toluene serves as a “spreading solution” to help control the atomic cluster solution film thickness on the surface.

In conclusion, ordered arrays of nanoparticles or nanowires were formed from atomic Au cluster solution. Arrays with hexagonal and square symmetries of round and square nanoparticles were selectively formed by controlling the substrate temperature and solvent composition. It was shown that definition of the array lattice points precedes complete formation of the particles, ruling out an entropy-driven “hard sphere”-type self-assembly mechanism. We suggest that a synergy of three temperature-dependent processes (structured hydrodynamics and

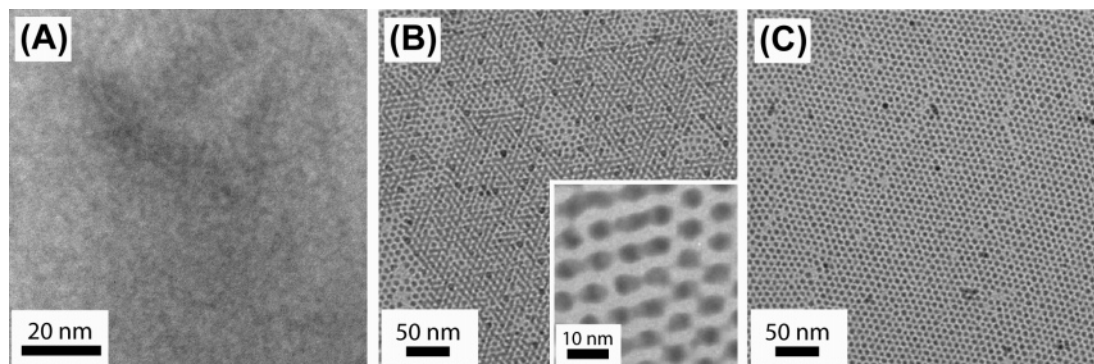


Figure 4. TEM images of (A) a sample dried at room temperature (no heating), (B) sample with substrate heated at 95 °C for 4 min, and (C) for 6 min. The inset in panel B shows the same sample under higher magnification.

amphiphilic molecule—molecule and molecule—surface interactions and structuring) is occurring. More precisely controlled heating and evaporation conditions are required to establish the operative mechanism. These studies are in progress.

Acknowledgment. We thank the National Science Foundation (CHE-0616663) for primary financial support. We also acknowledge central facilities support from the University of Chicago's NSF sponsored Materials Research Science and Engineering Center (MRSEC; DMR-0213745). P.L.R. and N.F.S. acknowledge a grant from the Camille and Henry Dreyfus Foundation. N.F.S. thanks the John F. Guggenheim Memorial Foundation for a fellowship.

References and Notes

- (1) Kawabata, A.; Kubo, R. *J. Phys. Soc. Jpn.* **1966**, *21*, 1765.
- (2) El-Sayed, M. A. *Acc. Chem. Res.* **2001**, *34*, 257.
- (3) Barnes, W. L.; Dereux, A.; Ebbesen, T. W. *Nature* **2003**, *424*, 824.
- (4) Pendry, J. P. *Science* **1999**, *285*, 1687.
- (5) Alivisatos, P. *Nat. Biotechnol.* **2004**, *22*, 47.
- (6) Taton, T. A.; Mirkin, C. A.; Letsinger, R. L. *Science* **2000**, *289*, 1757.
- (7) Lewis, L. N. *Chem. Rev.* **1993**, *93*, 2693.
- (8) Haruta, M. *Nature* **2005**, *437*, 1098.
- (9) Murray, C. B.; Kagan, C. R.; Bawendi, M. G. *Annu. Rev. Mater. Sci.* **2000**, *30*, 545.
- (10) Lin, X.-M.; Jaeger, H. M.; Sorensen, C. M.; Klabunde, K. J. *J. Phys. Chem. B* **2001**, *105*, 3353.
- (11) Shevchenko, E. V.; Talapin, D. V.; Murray, C. B.; O'Brien, S. J. *Am. Chem. Soc.* **2006**, *128*, 3620.
- (12) Hulteen, J. C.; Van Duyne, R. P. *J. Vac. Sci. Technol., A* **1995**, *13*, 1553.
- (13) Haynes, C. L.; Van Duyne, R. P. *J. Phys. Chem. B* **2001**, *105*, 5599.
- (14) Gotschy, W.; Vonmetz, K.; Leitner, A.; Aussenegg, F. R. *Appl. Phys. B* **1996**, *63*, 381.
- (15) Park, M.; Harrison, C.; Chaikin, P. M.; Register, R. A.; Adamson, D. H. *Science* **1997**, *276*, 1401.
- (16) Yin, A. J.; Li, J.; Jian, W.; Bennett, A. J.; Xu, J. M. *App. Phys. Lett.* **2001**, *79*, 1039.
- (17) Jin, R.; Egusa, S.; Scherer, N. F. *J. Am. Chem. Soc.* **2004**, *126*, 9900.
- (18) Zheng, J.; Zhang, C.; Dickson, R. M. *Phys. Rev. Lett.* **2004**, *93*, 077402.
- (19) Chen, S.; Ingram, R. S.; Hostetler, M. J.; Pietron, J. J.; Murray, R. W.; Schaaff, T. G.; Khoury, J. T.; Alvarez, M. M.; Whetten, R. L. *Science* **1998**, *280*, 2098.
- (20) Lin, X. M.; Wang, G. M.; Sorensen, C. M.; Klabunde, K. J. *J. Phys. Chem. B* **1999**, *103*, 5488.
- (21) Lin, X. M.; Sorensen, C. M.; Klabunde, K. J. *Chem. Mater.* **1999**, *11*, 198.
- (22) Egusa, S. Ph.D. Thesis, University of Chicago, 2005.
- (23) Several other solvents used for dilution were found to yield particle arrays: toluene, hexane, acetone, and methanol. Toluene was found to most reliably give particle array formation.
- (24) The histograms were obtained by thresholding and defining the particle contour in the TEM images.
- (25) Note that array formation does not occur for hexanethiol solution presumably because of the significantly lower boiling point (hexanethiol = 151 °C, octanethiol = 199 °C, dodecanethiol = 265 °C) and consequently too rapid evaporation.
- (26) Pusey, P. N.; van Megen, W. *Nature* **1986**, *320*, 340.
- (27) Wong, S.; Kitaev, V.; Ozin, G. A. *J. Am. Chem. Soc.* **2003**, *125*, 15589.
- (28) Bolhuis, P. G.; Frenkel, D.; Mau, S.-C.; Huse, D. A. *Nature* **1997**, *388*, 235.
- (29) Chandrasekhar, S. *Hydrodynamic and Hydromagnetic Stability*; Clarendon Press: Oxford, 1961.
- (30) Bodenschatz, E.; Pesch, W.; Ahlers, G. *Annu. Rev. Fluid Mech.* **2000**, *32*, 709.
- (31) Stowell, C. A.; Korgel, B. A. *Nano. Lett.* **2001**, *1*, 595.
- (32) Koschmieder, E. L. *Benard Cells and Taylor Vortices*; Cambridge University Press: Cambridge, 1993.
- (33) Yabu, H.; Tanaka, M.; Ijro, K.; Shimomura, M. *Langmuir* **2003**, *19*, 6297.
- (34) Srinivasarao, M.; Collings, D.; Philips, A.; Patel, S. *Science* **2001**, *292*, 79.
- (35) Widawski, G.; Rawiso, M.; Francois, B. *Nature* **1994**, *369*, 387.
- (36) Ravlv, U.; Laurat, P.; Klein, J. *Nature* **2001**, *413*, 51.
- (37) Chan, D. Y. C.; Horn, R. G. *J. Chem. Phys.* **1985**, *83*, 5311.
- (38) Gee, M. L.; McGuigan, P. M.; Israelachvili, J. N.; Homola, A. M. *J. Chem. Phys.* **1990**, *93*, 1895.
- (39) Love, J. C.; Estroff, L. A.; Kriebel, J. K.; Nuzzo, R. G.; Whitesides, G. M. *Chem. Rev.* **2005**, *105*, 1103.
- (40) Guo, Q.; Sun, X.; Palmer, R. E. *Phys. Rev. B* **2005**, *71*, 035406.
- (41) Schonenberger, C.; Jorritsma, J.; Sondag-Huethorst, A. M.; Fokkink, G. J. *J. Phys. Chem.* **1995**, *99*, 3259.
- (42) Luzzati, V.; Delacroix, H.; Gulik, A. *J. Phys. II France* **1996**, *6*, 405.
- (43) Adams, M.; Dogic, Z.; Keller, S. L.; Fraden, S. *Nature* **1998**, *393*, 349.
- (44) Kresge, C. T.; Leonowicz, M. E.; Roth, W. J.; Vartuli, J. C.; Beck, J. S. *Nature* **1992**, *359*, 710.
- (45) Hosoi, A. E.; Kogan, D.; Devereaux, C. E.; Bernoff, A. J.; Baker, S. M. *Phys. Rev. Lett.* **2005**, *95*, 037801.